Virchows Archiv (2019) 475:519–525
https://doi.org/10.1007/s00428-019-02619-4

BRIEF REPORT

SOX11 expression in a case of papillary thyroid carcinoma with fibromatosis/fasciitis-like stroma containing *BRAF* c.1799_1801delTGA and *CTNNB1* c.133T>C mutations

Soon Boon Justin Wong[1,2] · Min En Nga[1] · Michal Michal[3] · Tomas Vanecek[4] · Ju Ee Seet[5] · Fredrik Petersson[1,5]

Received: 27 February 2019 / Revised: 6 June 2019 / Accepted: 9 July 2019 / Published online: 20 July 2019

Abstract
We describe a case of papillary thyroid carcinoma with fibromatosis/fasciitis-like stroma (PTC-FLS) that contained the rare *BRAF* c.1799_1801delTGA (p.V600_K601delinsE) mutation, which has not previously been reported in this tumour, as well as the *CTNNB1* c.133T>C (p.S45P) mutation. We also report the novel observation that spindle cells of the mesenchymal component exhibit diffuse nuclear but not cytoplasmic expression of SOX11, whereas the malignant epithelial cells did not. This suggests that immunoreactivity for SOX11 can be an alternative diagnostic tool for evaluating cases of PTC-FLS where the nuclear expression of β-catenin is ambiguous.

Keywords Papillary thyroid carcinoma · Fibromatosis/fasciitis-like stroma · SOX11 · β-Catenin · BRAF · Mutation

Introduction

Of the morphologic variants of papillary thyroid carcinoma (PTC), some pose diagnostic challenges because of their rarity. One of the most uncommon variants of PTC displays biphasic morphology where the carcinomatous component is associated with a mesenchymal proliferation of spindled cells that has a fibromatosis/fasciitis-like appearance, and is thus referred to as PTC with fibromatosis/fasciitis-like stroma (PTC-FLS). Each of these two components harbours distinct activating mutations within oncogenes—*CTNNB1* in the mesenchymal component, and *BRAF* in the PTC component. Herein, we summarise existing data on the range of mutations that have been observed in the carcinomatous and mesenchymal components, and report a case of PTC-FLS with a *BRAF* c.1799_1801delTGA (p.V600_K601delinsE) mutation, which is a hitherto unreported genetic alteration in PTC-FLS. Our finding thus extends the range of documented *BRAF* mutations in this tumour.

✉ Fredrik Petersson
fredrikpetersson@live.se

[1] Department of Pathology, National University Hospital, Singapore, Singapore

[2] Department of Microbiology and Immunology, National University of Singapore, Singapore, Singapore

[3] Department of Pathology, Faculty of Medicine in Plzen, Charles University, Plzen, Czech Republic

[4] Molecular and Genetic Laboratory, Biopticka Laboratory Ltd., Plzen, Czech Republic

[5] Department of Pathology, National University Health System, 5 Lower Kent Ridge Road, Singapore 119074, Singapore

Case report

Clinical history

A 58-year-old Chinese male presented with a 2-month history of a painless enlarging neck lump. There was no dysphagia or hoarseness. Physical examination revealed a firm 5-cm nodule within the left thyroid lobe. The cervical lymph nodes were not enlarged. Ultrasonography showed two solid, heterogeneous, hypoechoic thyroid nodules with internal vascularity, one replacing most of the left lobe, the other in the upper pole of the right lobe. Fine needle aspiration (FNA) of both nodules was performed.

Cytology

Left lobe tumour (tumour #1): The smears were cellular and showed sheets of follicular cells with some microfollicles (Fig. 1a). Nuclear crowding, nuclear grooving and a few

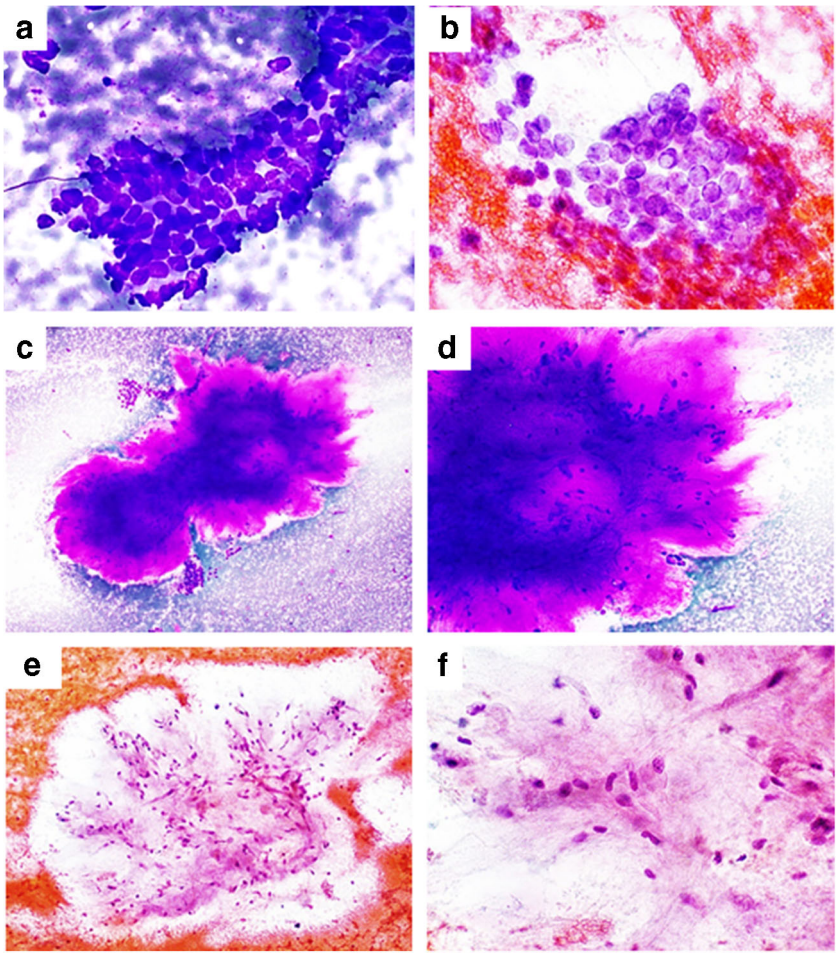

Fig. 1 Biphasic cytologic features of left thyroid lobe 5.0 cm nodule. **a** Crowded sheet of follicular cells (Hemacolor stain, × 200). **b** Follicular cells with chromatin clearing, nuclear grooves and intranuclear cytoplasmic pseudo-inclusions (Papanicolaou stain, × 600). **c–f** Metachromatic fibrillary stromal fragments containing spindled mesenchymal cells. The spindled cells contained elongated oval nuclei with dispersed chromatin and indistinct nucleoli; significant nuclear atypia was not seen, and mitotic figures were not identified (**c** and **d**: Hemacolor stain, × 40 and × 200, respectively; **e** and **f**: Papanicolaou stain, × 100 and × 400, respectively)

intranuclear pseudoinclusions were seen (Fig. 1b). In addition, there were fragments of metachromatic myxofibrillary stroma (Figs. 1c–f). This sample was reported as "Suspicious for PTC".

Right lobe tumour (tumour #2): The smears showed typical cytological features of PTC without the stroma seen in tumour #1. This sample was reported as "PTC".

Histopathology

The patient underwent total thyroidectomy with central compartment lymph node dissection. The resected thyroid gland contained two grossly identifiable tumours.

Left lobe tumour (tumour #1): A whitish tumour measuring 5.0 × 3.0 × 2.8 cm replaced most of the left lobe (Fig. 2a). This tumour was unencapsulated, and biphasic in composition, with a minor component composed of clusters of neoplastic follicular cells (approximately 25% of tumour volume) intermixed with an exuberant spindle cell component that did not show significant nuclear atypia (75% of tumour volume) (Fig. 2b). The epithelial component showed features compatible with papillary thyroid carcinoma (Fig. 2c, d). Portions of the mesenchymal component displayed fasciitis-like features (Fig. 2e, f), whereas other areas resembled fibromatosis (Fig. 2g, h). Mitotic activity was scant in both epithelial and mesenchymal components. No tumour necrosis, squamous morules or psammoma bodies were identified. A diagnosis of PTC with fibromatosis/fasciitis-like stroma (PTC-FLS) was made. Foci of vascular invasion were identified, featuring both epithelial and mesenchymal components (Fig. 3a). Tumour containing both epithelial and mesenchymal elements infiltrated into perithyroidal skeletal muscle, and the surgical resection margin was focally involved by both tumour components.

Right lobe tumour (tumour #2): A whitish nodule in the superior pole of the right lobe measuring 1.9 cm in greatest extent. The histological features were compatible with classical PTC, with invasion into perithyroidal skeletal muscle and focal involvement of the circumferential resection margin.

There were also multiple foci of papillary microcarcinoma in both thyroid lobes and the isthmus. Neither tumour #2 nor the foci of papillary microcarcinoma contained the fibromatosis/fasciitis-like mesenchymal component seen in tumour #1.

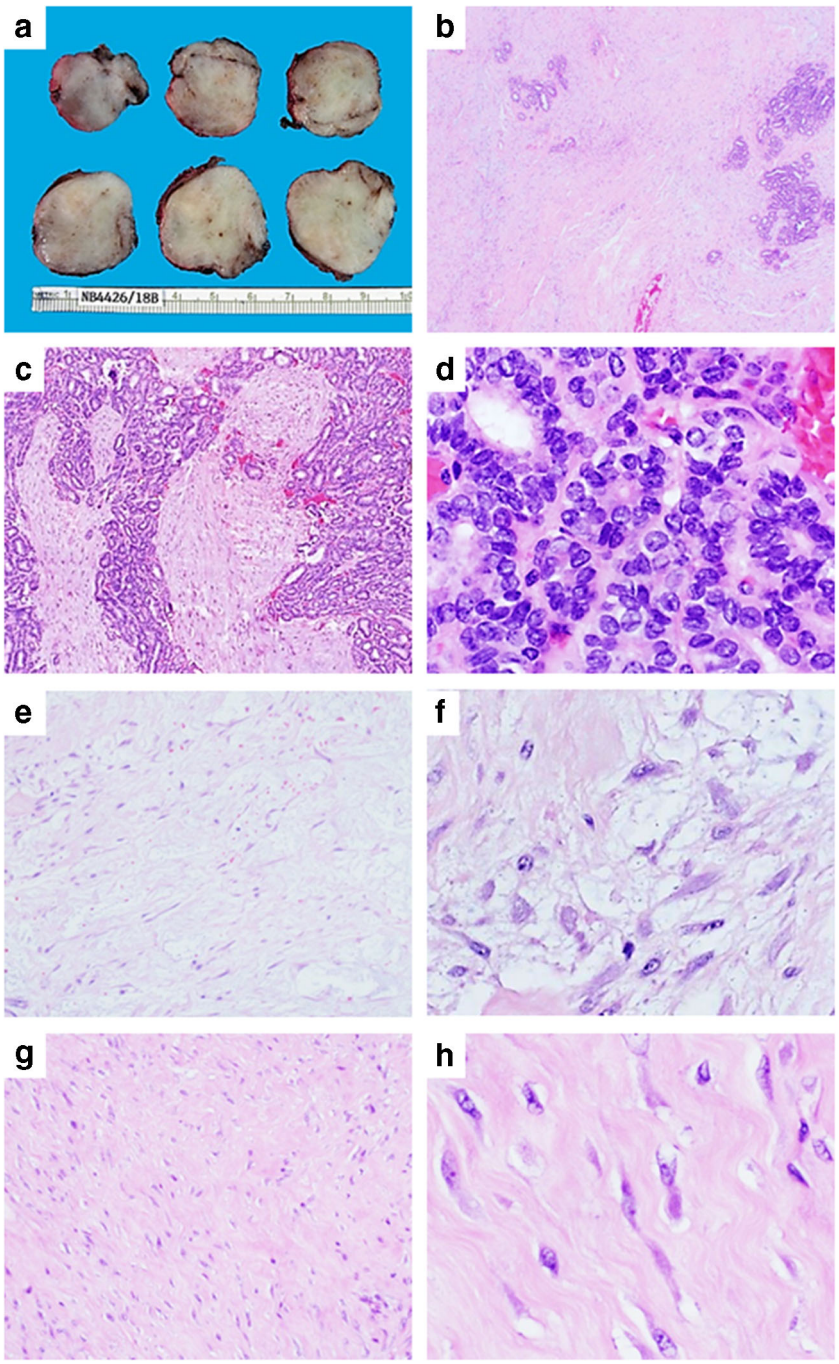

Fig. 2 Gross and histologic features of the left thyroid lobe 5.0 cm tumour. **a** The tumour was unusually pale in colour and rubbery in consistency. It largely replaced the entire lobe and abutted the circumferential margin. **b** Most of the tumour consisted of a mesenchymal proliferation, with a smaller epithelial component (H&E, × 20). **c**, **d** The epithelial component was composed of distorted follicles and papillary structures, which were lined by cuboidal or columnar cells with nuclear features of PTC, namely, enlarged, crowded, oval-shaped, optically clear nuclei with prominent nuclear grooves and occasional intranuclear cytoplasmic pseudo-inclusions (H&E, × 40 and × 400, respectively). **e**, **f** In areas with fasciitis-like features, the mesenchymal component contained plump, spindled to stellate cells, which were loosely arranged within myxoid extracellular material (H&E, × 100 and × 400, respectively). **g**, **h** Other areas appeared more cellular, and contained streaming fascicles of bland spindled cells associated with eosinophilic bundles of collagen fibres, resembling fibromatosis (H&E, × 100 and × 400, respectively)

Five out of seven cervical lymph nodes contained metastatic carcinoma. The largest metastatic deposit measured 0.4 cm, with extranodal extension. Nodal metastases did not contain a fibromatosis/fasciitis-like mesenchymal component.

Immunohistochemistry

β-Catenin Cells in the fibromatosis/fasciitis-like mesenchymal component of tumour #1 showed granular cytoplasmic staining with perinuclear accentuation (Fig. 3b). Assessment for nuclear localisation of β-catenin expression was challenging, particularly when strong cytoplasmic β-catenin expression masked the underlying slender fusiform nucleus. Despite careful evaluation, no definite nuclear staining was observed. PTC follicular cells showed membranous and granular cytoplasmic β-catenin expression.

SOX11 Stromal cells in the fasciitis- and fibromatosis-like mesenchymal components of tumour #1 both showed nuclear expression of SOX11 (Fig. 3c, d). PTC follicular cells were

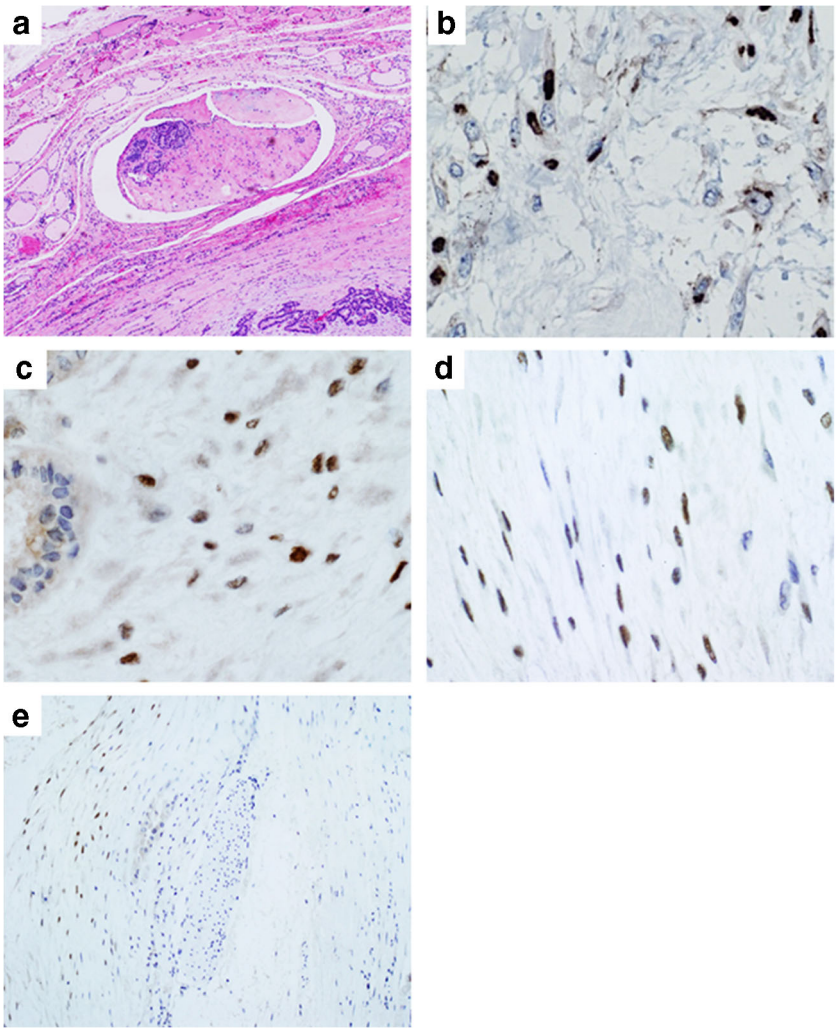

Fig. 3 Lymphovascular tumour emboli, and immunohistochemical features of the left lobe 5.0 cm tumour. **a** Foci of lymphovascular tumour emboli were identified, containing both epithelial and mesenchymal components of the tumour (H&E, × 40). **b** There was granular cytoplasmic expression of β-catenin within spindle cells of the mesenchymal component (× 400). Expression of β-catenin was determined by immunohistochemistry using antibody clone β-catenin-1 (Dako, 1:100 dilution). **c**, **d** Spindled cells of the mesenchymal component showed nuclear but not cytoplasmic expression of SOX11 in the fasciitis-like areas (**c**, × 400), as well as the fibromatosis-like areas (**d**, × 400), whereas follicular cells were negative (**c**, left side of field). **e** There was also no expression of SOX11 within fibroblasts of the perithyroidal connective tissue (right side of field) that surrounded the tumour (left side of field, × 100). Expression of SOX11 was determined by immunohistochemistry using antibody clone MRQ-58 (Cell Marque, 1:50 dilution)

negative (Fig. 3c, e), as were fibroblasts in non-neoplastic perithyroidal connective tissue surrounding the tumour (Fig. 3e).

Molecular analysis

DNA was isolated from formalin-fixed paraffin-embedded tissue using Qiagen DNA mini kit, purified with AMPure XP (Beckman Coulter, Brea, CA, USA), and quantified using Qubit DNA HS (Thermo Fisher Scientific, Waltham, MA, USA). DNA integrity was evaluated by PCR amplification of several control sequences of lengths 100–600 base pairs. The VariantPlex solid tumour kit (ArcherDX, Boulder, CO, USA) was used for mutational analysis of 67 gene targets. DNA libraries were constructed using the manufacturer's protocol and sequenced on NextSeq 500 (Illumina, San Diego, CA, USA) with at least 2.5 million reads per sample. Data analysis was performed using Archer Analysis software (version 5.1.7). DNA from tumour #1 analysed in this manner showed a mutant *CTNNB1* c.133T>C allele (corresponding to p.S45P), and a *BRAF* c.1799_1801delTGA mutation (corresponding to p.V600_K601delinsE). Sanger sequencing confirmed the c.133T>C allele within exon 3 of *CTNNB1* in tumour #1.

Post-operative course

The patient received radioiodine, and has been recurrence-free in 8 months of clinical follow-up since the operation. Distant metastases have not been detected.

Discussion

Papillary thyroid carcinoma with fibromatosis/fasciitis-like stroma is a rare variant of PTC first described by Ostrowski et al. [9]. The often exuberant mesenchymal spindle cell component of PTC-FLS morphologically resembles desmoid-type fibromatosis (DTF), a myofibroblastic proliferation of deep soft tissue that characteristically exhibits aberrant nuclear expression of β-catenin [11]. Hence, several investigators have

evaluated β-catenin expression in PTC-FLS [2, 8, 10, 12, 13, 15]. To date, 17 out of 19 previously reported cases of PTC-FLS exhibit aberrant nuclear β-catenin expression (Table 1). However, a thorough assessment of the current case failed to show convincing evidence of nuclear β-catenin expression within the spindled cells, even though an underlying mutation

Table 1 Summary of molecularly characterized cases of PTC-FLS in the literature

	β catenin expression pattern in mesenchymal component	*CTNNB1* mutation status	*BRAF* mutation status
Na K. et al. 2013	1 out of 1 case with aberrant nuclear and cytoplasmic immunoreactivity	Not done	Not done
Ginter P. et al. 2015	1 out of 1 case with aberrant nuclear and cytoplasmic immunoreactivity	Not done	p.V600E mutation detected in one case, but methodology not stated
Rebecchini C. et al. 2017	2 out of 2 cases showed aberrant nuclear and cytoplasmic immunoreactivity	Heterozygous c.133T>C (p.S45P) mutation detected in 2 out of 2 cases by DNA sequencing	Heterozygous c.1799T>A (p.V600E) mutation detected in 2 out of 2 cases by DNA sequencing
Takada N. et al. 2017	12 out of 14 cases showed nuclear and cytoplasmic immunoreactivity. The 2 remaining cases showed membranous reactivity	Not done	Not done
Takada N. et al. 2018	8 out of 8 cases with nuclear and cytoplasmic immunoreactivity (possibly from the same patient pool as Takada N. et al. 2017)	c.121A>G (p.T41A) mutation detected in 1 out of 8 cases by DNA sequencing	8 out of 8 cases showed immunoreactivity for BRAF (p.V600E) 7 out of 7 cases tested by DNA sequencing contained the c.1799T>A (p.V600E) mutation
Zhou L. et al. 2018	1 out of 1 case with aberrant nuclear immunoreactivity (assessed in the recurrent tumour)	Heterozygous c.134C>T (p.S45F) mutation detected by DNA sequencing in the recurrent spindle cell tumour (for the primary PTC-FLS tumour: mutation described in text but data not shown)	Not done
This report	1 out of 1 case with granular cytoplasmic expression pattern and perinuclear accentuation. No definite nuclear immunoreactivity	c.133T>C (p.S45P) mutation detected using the VariantPlex solid tumour hotspot NGS panel (ArcherDx), and confirmed by DNA sequencing	1 out of 1 case with the c.1799_1801delTGA (p.V600_K601delinsE) mutation detected using the VariantPlex solid tumour hotspot NGS panel (ArcherDx)

in *CTNNB1* was detected using two independent molecular methods. Thus, we sought to identify additional immunohistochemical markers that might be useful for supporting a diagnosis of PTC-FLS. Aberrant SOX11 expression has been observed in DTF [7]. We now report the novel observation that spindle cells within the mesenchymal component of PTC-FLS also demonstrate nuclear expression of SOX11, whereas the carcinomatous component and fibroblasts within perithyroidal connective tissue do not express this marker. In contrast to the immunohistochemical detection of β-catenin, which can be difficult to interpret particularly when cytoplasmic staining obscures the underlying nucleus, SOX11 immunoreactivity is a clean nuclear signal devoid of cytoplasmic background staining. These features suggest that SOX11 expression can be a novel tool for corroborating the diagnosis of PTC-FLS in cases that show equivocal nuclear staining of β-catenin. Our findings also suggest immunohistochemical staining with β-catenin and SOX11 in cell block material derived from FNA biopsies may aid in the pre-operative diagnosis of this rare PTC variant, thereby facilitating appropriate and timely treatment.

Activating *CTNNB1* mutations have been found in up to 88% of sporadic DTF, but a limited mutational spectrum has been observed, predominantly involving c.121A>G (p.T41A), c.134C>T (p.S45F) or c.133C>T (p.S45P) [11]. In comparison, *CTNNB1* mutations occur in a smaller proportion of PTC-FLS: 5 out of 12 instances including the current case (42%, Table 1). To date, only p.T41A, p.S45F and p.S45P mutations have been described in PTC-FLS; the most common of these is p.S45P, present in 3 out of 5 instances including the current case (60%, Table 1). In contrast, the frequency of p.S45P in *CTNNB1*-mutated DTF is much lower (up to 12%, [6]). A correlation between β-catenin mutant status and recurrence-free survival has been reported in some, but not all, studies of sporadic DTF. The p.S45F mutation, in particular, has been associated with increased risk of recurrence [5]. Whether the same will hold true for PTC-FLS is still unclear. The sole reported case of PTC-FLS with local recurrence of the spindle cell component contained the p.S45F mutation [15].

BRAF mutations are the most common genetic alterations in PTC (geographic variation ranging from 32 to 87%; the prevalence is 56% at our institution [3]). Several activating *BRAF* mutations have been described, but the c.1799T>A (p.V600E) mutation is the most frequently encountered. While activating BRAF mutations is common but not universal in finding for PTC in general, all 9 previously reported cases of PTC-FLS where DNA analysis was carried out contain the c.1799T>A (p.V600E) mutation (Table 1). The current case is the exception, being the first reported case of PTC-FLS with the *BRAF* c.1799_1801delTGA (p.V600_K601delinsE) mutation. This uncommon mutation occurs in up to 0.86% of *BRAF* mutant PTC [1]. Similar to the p.V600E mutation, p.V600_K601delinsE results in constitutive activation of the downstream MAPK signalling pathway [1, 4]. Since there appears to be universal occurrence of *BRAF*-activating mutations in PTC-FLS, and proliferation of tumour-associated fibroblasts is increased in classical PTC with *BRAF* p.V600E mutation compared with classical PTC containing wild-type *BRAF* [14], we speculate that dysregulated activation of signalling pathways downstream from *BRAF* within the PTC component might be essential for triggering the exuberant mesenchymal spindle cell proliferation that is an inherent feature of PTC-FLS.

Authors' contributions SBJW: tissue sampling, histological analysis, interpretation of data, literature review, drafting and review of manuscript. MEN: histological analysis, interpretation of data and review of manuscript. TV and MM: analysis of molecular features. JES: cytological analysis and review of manuscript. FP: histological analysis, interpretation of data, literature review, review of manuscript, study supervision, study design, decision to submit and publish the manuscript. All authors gave the final approval for publication.

Compliance with ethical standards

Conflict of interest The authors declare that they have no conflict of interest.

Ethical standard This is a brief report on a novel and unique case of diagnostic interest; it is not a research project; there is no human or animal participant(s). It is our institution's policy not to require consent for studies up to two subjects.

References

1. Barollo S, Pezzani R, Cristiani A, Redaelli M, Zambonin L, Rubin B, Bertazza L, Zane M, Mucignat-Caretta C, Bulfone A, Pennelli G, Casal Ide E, Pelizzo MR, Mantero F, Moro S, Mian C (2014) Prevalence, tumorigenic role, and biochemical implications of rare BRAF alterations. Thyroid 24:809–819. https://doi.org/10.1089/thy.2013.0403
2. Ginter PS, Scognamiglio T (2015) Papillary thyroid carcinoma with nodular fasciitis-like stroma: a usual entity with distinctive morphology. Int J Surg Pathol 23:305–307. https://doi.org/10.1177/1066896915570362
3. Goh X, Lum J, Yang SP, Chionh SB, Koay E, Chiu L, Parameswaran R, Ngiam KY, Loh TKS, Nga ME, Lim CM (2019) BRAF mutation in papillary thyroid cancer-prevalence and clinical correlation in a South-East Asian cohort. Clin Otolaryngol 44:114–123. https://doi.org/10.1111/coa.13238
4. Hou P, Liu D, Xing M (2007) Functional characterization of the T1799-1801del and A1799-1816ins BRAF mutations in papillary thyroid cancer. Cell Cycle 6:377–379. https://doi.org/10.4161/cc.6.3.3818
5. Lazar AJ, Tuvin D, Hajibashi S, Habeeb S, Bolshakov S, Mayordomo-Aranda E, Warneke CL, Lopez-Terrada D, Pollock RE, Lev D (2008) Specific mutations in the beta-catenin gene (CTNNB1) correlate with local recurrence in sporadic desmoid tumors. Am J Pathol 173:1518–1527. https://doi.org/10.2353/ajpath.2008.080475
6. Le Guellec S, Soubeyran I, Rochaix P, Filleron T, Neuville A, Hostein I, Coindre J-M (2012) CTNNB1 mutation analysis is a useful tool for the diagnosis of desmoid tumors: a study of 260

desmoid tumors and 191 potential morphologic mimics. Mod Pathol 25:1551–1558. https://doi.org/10.1038/modpathol.2012.115
7. Misemer BS, Skubitz AP, Carlos Manivel J, Schmechel SC, Cheng EY, Henriksen JC, Koopmeiners JS, Corless CL, Skubitz KM (2014) Expression of FAP, ADAM12, WISP1, and SOX11 is heterogeneous in aggressive fibromatosis and spatially relates to the histologic features of tumor activity. Cancer Med 3:81–90. https://doi.org/10.1002/cam4.160
8. Na KY, Kim HS, Sung JY, Park WS, Kim YW (2013) Papillary carcinoma of the thyroid gland with nodular fasciitis-like stroma. Kor J Pathol 47:167–171. https://doi.org/10.4132/KoreanJPathol.2013.47.2.167
9. Ostrowski MA, Moffat FL, Asa SL, Rostein LE, Chamberlain D (1989) Myxomatous change in papillary carcinoma of the thyroid. Surg Pathol 2:249–256
10. Rebecchini C, Nobile A, Piana S, Sarro R, Bisig B, Gerasimos SP, Saglietti C, Matter M, Marino L, Bongiovanni M (2017) Papillary thyroid carcinoma with nodular fasciitis-like stroma and beta-catenin mutations should be renamed papillary thyroid carcinoma with desmoid-type fibromatosis. Mod Pathol 30:236–245. https://doi.org/10.1038/modpathol.2016.173
11. Skubitz KM (2017) Biology and treatment of aggressive fibromatosis or desmoid tumor. Mayo Clin Proc 92:947–964. https://doi.org/10.1016/j.mayocp.2017.02.012
12. Takada N, Hirokawa M, Ito M, Ito A, Suzuki A, Higuchi M, Kuma S, Hayashi T, Kishikawa M, Horikawa S, Miyauchi A (2017) Papillary thyroid carcinoma with desmoid-type fibromatosis: a clinical, pathological, and immunohistochemical study of 14 cases. Endocr J 64:1017–1023. https://doi.org/10.1507/endocrj.EJ17-0242
13. Takada N, Mussazhanova Z, Hirokawa M, Nakashima M, Miyauchi A (2018) Immunohistochemical and molecular analyses focusing on mesenchymal cells in papillary thyroid carcinoma with desmoid-type fibromatosis. Pathobiology 85:300–303. https://doi.org/10.1159/000492117
14. Tarabichi M, Antoniou A, Le Pennec S, Gacquer D, de Saint AN, Craciun L, Cielen T, Laios I, Larsimont D, Andry G, Dumont JE, Maenhaut C, Detours V (2018) Distinctive desmoplastic 3D morphology associated with BRAFV600E in papillary thyroid cancers. J Clin Endocrinol Metab 103:1102–1111. https://doi.org/10.1210/jc.2017-02279
15. Zhou L, Shi L, Jiang Z, Xie L (2018) Papillary thyroid carcinoma with nodular-fasciitis-like stroma and beta-catenin gene mutations: report of a recurrent case. Int J Clin Exp Pathol 11:2879–2883